NO reduction with acetaldehyde on alumina-supported Pd–Mo catalysts

L.F. de Mello, F.B. Noronha [1], M. Schmal [*]

NUCAT-PEQ-COPPE, Universidade Federal do Rio de Janeiro, Ilha do Fundão, C.P. 68502, CEP 21941, Rio de Janeiro, Brazil

Abstract

The reduction of NO with acetaldehyde on alumina-supported Pd, Mo, and Pd–Mo catalysts was studied. Two Mo loadings were used (8 and 20%), and the Pd–8% Mo/Al_2O_3 catalyst was the most active for NO conversion. Temperature-programmed desorption and infrared measurements of adsorbed acetaldehyde indicated that acetate species are probably an important reaction intermediate. The presence of Pd in close contact with Mo favors formation of the acetate species, which could explain the higher activity for the Pd8Mo sample. The 20% Mo loading produced bulk MoO_3, which covered part of the Pd sites, and thus the activity for this catalyst was lower.
© 2006 Elsevier Inc. All rights reserved.

Keywords: Palladium; Molybdenum; TPD and reactions; NO; Acetaldehyde

1. Introduction

Recently, due to economical and pollution control considerations, the use of alcohols and ethers as fuel additives for gasoline powered vehicles is spreading [1]. Methyl *tert*-butyl ether (MTBE), methanol, and ethanol are the most commonly used oxygenates. These compounds reduce the emission of some pollutants, including olefins, SO_x and soot, but increase the amount of other unwanted products. The addition of ethanol, for instance, increases the direct emissions of unburned ethanol and aldehydes (acetaldehyde and formaldehyde) to the atmosphere [2]. This problem is even greater in countries like Brazil, where there are two types of automotive fuel: pure, hydrated ethanol and a 20–25% (v/v) ethanol and gasoline blend. Some early technical research [2,3] showed that adding 22% of ethanol to pure gasoline produced an increase of up to 25% NO_x and 200% acetaldehyde in the exhaust system of vehicles [2]. Another study [3] showed that for ethanol-fuled vehicles, emission of aldehydes may reach as high as 7.2 wt% of total organic compounds in the exhaust system. Besides the

potential carcinogenic effects of aldehydes, such products may also react on the atmosphere, producing other toxic compounds and contributing to the formation of photochemical smog [4]. Thus, such systems need better emission control using adequate catalytic converters; for this purpose, fundamental information on the catalytic surface properties and processes is needed. It is important to understand the influence of oxygenated organic compounds in the exhaust system on the abatement of NO_x.

Some previous papers have presented fundamental research [5–8] regarding the adsorption properties and surface reaction of aldehydes on different catalysts. Cordi and Falconer [5] studied the reactivity of several volatile organic compounds, including acetaldehyde, on the surface of alumina-supported palladium catalysts using temperature-programmed desorption (TPD) and temperature-programmed oxidation (TPO) techniques. Idriss et al. [6] investigated the adsorption properties as well as the reactions of acetaldehyde on the surface of CeO_2-supported catalysts using TPD and infrared (IR) measurements.

The present paper continues a line of work on Pd–Mo/Al_2O_3 catalysts [9–13], which have been used to control the exhaust emissions of ethanol-fueled Brazilian vehicles [14]. Previous papers [9–11] have reported that adding MoO_3 to Pd/Al_2O_3 catalysts improved the NO activity with high selectivity to N_2 during the NO + CO reaction. According to Schmal et al. [9], the promoting effect of Mo is due to a redox mechanism in which the partially reduced molybdenum oxide surface adsorbs

* Corresponding author. Fax: +55 21 2906626.
 E-mail addresses: fabiobel@int.gov.br (F.B. Noronha),
schmal@peq.coppe.ufrj.br (M. Schmal).
 [1] Present address: Instituto Nacional de Tecnologia, INT, Av. Venezuela 82, CEP 20081-310, Rio de Janeiro, Brazil.

and decomposes the NO molecules (producing mainly N_2), while the oxygen from the NO is made available to the metallic palladium sites to oxidize the adsorbed CO molecules. The reaction of NO + ethanol on Pd–Mo catalysts has also been investigated in previous work [12,13]; the results indicated that formation of acetaldehyde is likely an important step in the reaction mechanism. According to that work, the dehydrogenation of ethanol to acetaldehyde would be the rate-determining step, which produces surface acetate species that react with adsorbed NO. Hence, it is important to study the interaction and also the reactivity of acetaldehyde with the catalytic surface, to better understand the influence of an organic oxygenate, such as acetaldehyde or ethanol, as a possible reducing agent of NO. More recently, the ethanol reaction with NO was studied with Pd/CeZrO$_2$ [13] and similar results were observed.

The present work focuses attention on the adsorption properties of acetaldehyde on the surface of Pd–Mo/Al$_2$O$_3$ catalysts and also on the reactivity of these catalysts for the NO + acetaldehyde reaction. The main techniques used were TPD, temperature-programmed surface reaction (TPSR), and IR spectroscopy of adsorbed acetaldehyde, as well as catalytic tests.

2. Experimental

2.1. Catalyst preparation

The 8% Mo and 20% Mo/Al$_2$O$_3$ catalysts were prepared by wet impregnation of γ-Al$_2$O$_3$ (Engelhard; BET area = 216 m^2/g) with an aqueous solution of $(NH_4)_6Mo_7O_{24}\cdot4H_2O$. The samples were dried at 383 K for 22 h and calcined under flowing air at 773 K for 2 h. Pd/Al$_2$O$_3$ and Pd–Mo/Al$_2$O$_3$ samples were prepared by wet impregnation of Al$_2$O$_3$ and Mo/Al$_2$O$_3$, respectively, with a solution of Pd(NO$_3$)$_2$ (Aldrich). The samples were then dried at 373 K and calcined under flowing air at 773 K for 2 h. Table 1 presents the nomenclature and composition of all catalysts.

2.2. Catalyst characterization

2.2.1. H$_2$ chemisorption

H$_2$ uptakes were measured in an Micromeritics ASAP 2000C instrument. Before the analyses, the samples were dehydrated at 423 K for 0.5 h. Then the catalysts were reduced at 773 K (at a rate of 5 K/min) in flowing H$_2$ (30 cm^3/min) for 1 h. After reduction, the samples were evacuated for 1 h at the reduction temperature and cooled to the adsorption temperature under vacuum. Irreversible uptakes were determined from dual isotherms measured for hydrogen (at 343 K) [15].

2.2.2. TPD

The TPD experiments for adsorbed acetaldehyde were performed in a glass microreactor coupled to a quadrupole mass spectrometer (Prisma, Balzers). A Quadstar analytical system was used to select and record different signal intensities of masses as functions of temperature. Before the TPD analyses, all samples were purged under helium flow (50 cm^3/min) from room temperature up to 823 K at a heating rate of 10 K/min. The samples were then cooled to room temperature and reduced under flowing H$_2$ (30 cm^3/min) up to 773 K (5 K/min), then kept at that temperature for 2 h. After reduction, the system was outgassed with helium flow at the reduction temperature for 30 min and cooled to room temperature. The adsorption of acetaldehyde was accomplished through pulses of an acetaldehyde/He mixture obtained by passing He through a saturator containing acetaldehyde at 278 K. After adsorption, the catalyst sample was heated at 20 K/min up to 823 K in flowing helium (50 cm^3/min).

To better understand and quantify the TPD results, the mass spectrometer was calibrated beforehand. The calibration consisted of experimentally determining the fragmentation pattern of acetaldehyde as well as of each individual product. The correction procedure to determine the distribution of the desorbed products has been described in detail elsewhere [12]. In general, the factors relating the main fragment of each product to the corresponding secondary fragments were determined, and then these factors were used to subtract the influence of two or more overlapping fragments of different products. The values of each factor are presented in Table 2.

2.2.3. TPSR

The TPSR experiments were done in a similar way to the TPD analysis. All samples were first purged with helium flow (50 cm^3/min) from room temperature up to 823 K (at a rate of 10 K/min), cooled back to room temperature, and reduced under flowing H$_2$ (30 cm^3/min) up to 773 K (at a rate of 5 K/min), then kept at that temperature for 2 h. After reduction, the system was purged with helium at the reduction temperature for 30 min and cooled to room temperature. Acetaldehyde was adsorbed at room temperature until saturation of the surface was achieved. After adsorption, the samples were purged with He, and a flow of a 1% NO/He mixture (50 cm^3/min) was passed as

Table 1
Catalyst nomenclature and composition

Catalyst	Nomen-clature	Pd loading (wt%)	Mo loading (wt%)	BET (m^2/g)
γ-Al$_2$O$_3$	Al$_2$O$_3$	–	–	216
8% Mo/Al$_2$O$_3$	8Mo	–	8.3	196
20% Mo/Al$_2$O$_3$	20Mo	–	18.6	173
1% Pd/Al$_2$O$_3$	Pd	0.69	–	213
1% Pd–8% Mo/Al$_2$O$_3$	Pd8Mo	0.63	8.3	185
1% Pd–20% Mo/Al$_2$O$_3$	Pd20Mo	0.60	17	162

Table 2
Major fragments of products desorbed during acetaldehyde TPD and intensity ratios of mass fragments

Products	Major fragments	Intensity ratios for mass fragments
CO	**28**	–
CO$_2$	**44**, 28	44/28 = 9.96
C$_2$H$_5$OH	**31**, 45, 27, 29	31/29 = 1.30
		31/27 = 2.45
C$_2$H$_4$O	**29**, 44	29/44 = 2.20

the temperature was raised at a rate of 20 K/min up to 823 K. The reaction products were monitored using a quadrupole mass spectrometer (Prisma, Balzers), as described previously [9,12]. Due to experimental complexity, TPSR experiments were performed only for the Pd/Al_2O_3, 8Mo, and Pd8Mo catalysts.

2.2.4. IR spectroscopy of adsorbed acetaldehyde

A Fourier transform IR (FTIR) spectrometer (Perkin Elmer 2000) was used to monitor the adsorption of acetaldehyde. The 25-mg samples were pressed into self-supported wafers, and all of the pretreatments were carried out in situ in a glass cell with CaF_2 windows. Before adsorption, the samples were reduced with H_2 at 773 K for 1 h. After evacuation at the reduction temperature for 1 h and cooling to room temperature, acetaldehyde was introduced into the cell at 298 K until saturation was achieved, followed by FTIR measurement under vacuum at 298 K. Then the samples were heated at different temperatures (373, 423, 473, 573, 673, and 773 K) under vacuum and spectra were recorded, with a resolution of 4 cm^{-1}.

2.3. Catalytic activity

The catalytic experiments were performed in a glass microreactor at atmospheric pressure. The 140-mg samples were pretreated in flowing helium (50 ml/min) at 823 K for 0.5 h and then reduced with pure H_2 at 773 K for 1 h. The feed mixture for the NO + acetaldehyde reaction consisted of 0.4% acetaldehyde/0.7% NO balanced with He at a flow rate of 250 ml/min (space velocity = 82,500 h^{-1}). To obtain the gas feed, a 0.97% NO/He (AGA) gas mixture was used. The acetaldehyde/He mixture was made by passing He through a saturator containing 99.995% pure acetaldehyde (Merck) at 265 K. The effluent was analyzed by gas chromatography (Chrompack with a thermal conductivity detector, a Chromosorb 102 column, and cryogen), and the reaction temperature was varied between 523 and 673 K.

The influence of the presence of oxygen was also studied in the present work. In this case a reaction feed mixture consisting of 0.4% acetaldehyde/0.6% NO/0.7% O_2 balanced with He at a flow rate of 250 ml/min was used. The reaction temperature was varied between 553 and 673 K. Sample weight, pretreatment conditions, and effluent analysis were the same as for the oxygen-free experiments.

3. Results

3.1. H_2 chemisorption

Table 3 gives the H_2 uptake for the chemisorption measurements on Pd, 8Mo, Pd8Mo, 20Mo, and Pd20Mo catalysts. The 8Mo and 20Mo catalysts showed very low H_2 uptake. The addition of molybdenum to the Pd/Al_2O_3 catalyst strongly decreased the amount of chemisorbed hydrogen.

3.2. IR spectroscopy of adsorbed acetaldehyde

The IR spectrum after adsorption of acetaldehyde on alumina (Fig. 1) showed, at room temperature, overlapping bands

Table 3
H_2 chemisorption

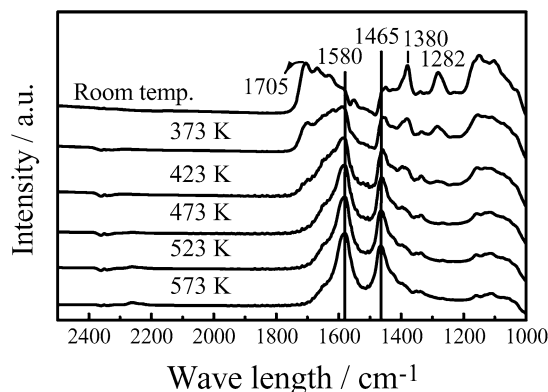| Sample	H_2 uptake ($\mu mol_{H_2}/g_{cat}$)
8Mo	0
20Mo	0.112
Pd	6.640
Pd8Mo	1.403
Pd20Mo	0.158

Fig. 1. IR spectra of adsorbed acetaldehyde on Al_2O_3.

at the 1000–1200 and 1590–1670 cm^{-1} regions, as well as bands at 1282, 1380, and 1705 cm^{-1}. Raskó and Kiss [8] studied the adsorption and surface reactions of acetaldehyde on TiO_2, CeO_2, and Al_2O_3 and found the following vibrational frequencies for molecularly adsorbed acetaldehyde: for the $\nu(CO)$ mode, TiO_2, 1729–1686 cm^{-1}; CeO_2, 1717–1706 cm^{-1}; and Al_2O_3, 1723–1694 cm^{-1}; for the $\delta(CH)$ mode, TiO_2, 1386–1372 cm^{-1}; CeO_2, 1378–1366 cm^{-1}; and Al_2O_3, 1380–1374 cm^{-1}. Besides the bands associated with adsorbed acetaldehyde, these authors also identified bands at 1663–1638 cm^{-1} [$\nu(C=O)$], 1596–1586 cm^{-1} [$\nu(C=C)$], 1260–1280 cm^{-1} [$\delta(CH)$], and 1173–1160 cm^{-1} [$\nu(C=C)$, $\rho(CH_3)$] which were attributed to adsorbed crotonaldehyde, and bands at 1079–1037 cm^{-1}, which were assigned to adsorbed ethoxy species.

Idriss et al. [6] studied the adsorption of acetaldehyde on reduced ceria and Pd/ceria catalysts and identified bands related to different species, including ethoxy species at 1376 cm^{-1} [$\delta(CH)$] and 1067 cm^{-1} [$\nu(CO)$]; crotonaldehyde at 1662 cm^{-1} [$\nu(CO)$], 1606 cm^{-1} [$\nu(C=C)$], 1404 cm^{-1} [$\delta(CH)$], 1160 cm^{-1} [$\nu(C=C)$, $\rho(CH_3)$], and 1108 cm^{-1} [$\nu(C=C)$]; and molecularly adsorbed acetaldehyde at 1715 cm^{-1}. Furthermore, Nagal and Gonzalez [7] made in situ IR measurements during the oxidation of acetaldehyde on Pt/SiO_2 catalysts and observed the presence of a band at 1722 cm^{-1}, which was attributed to the carbonyl group of adsorbed acetaldehyde.

In light of the foregoing observations, the bands observed after adsorption of acetaldehyde at room temperature on alumina possibly indicate the presence of the following adsorbed species: ethoxy (1000–1200 cm^{-1}, 1380 cm^{-1}), crotonaldehyde (1000–1200 cm^{-1}, 1590–1670 cm^{-1}, and 1282 cm^{-1}), and molecular acetaldehyde (1705 and 1380 cm^{-1}).

Fig. 2. IR spectra of adsorbed acetaldehyde on Pd/Al$_2$O$_3$.

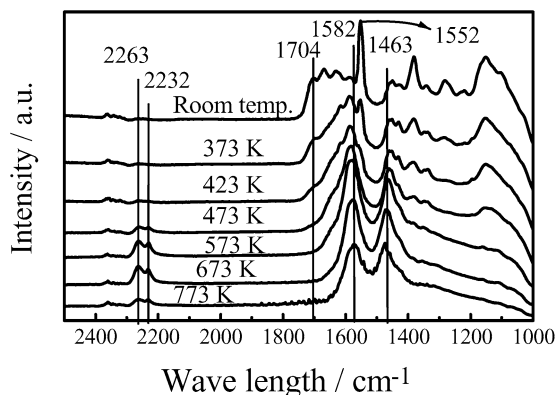Fig. 3. IR spectra of adsorbed acetaldehyde on 8Mo/Al$_2$O$_3$.

Fig. 4. IR spectra of adsorbed acetaldehyde on Pd8Mo/Al$_2$O$_3$.

As the temperature of the alumina sample increased, the intensity of the bands originally observed at room temperature decreased, and bands appeared at 1465 and 1580 cm^{-1}. These bands were attributed to the presence of acetate species, formed on acetaldehyde oxidation on surface oxygen sites (S–O). In fact, several other works have identified such acetate species after adsorption of both acetaldehyde as well as ethanol [6–8, 12,16,17].

At room temperature, the IR spectrum of adsorbed acetaldehyde on Pd/Al$_2$O$_3$ (Fig. 2) showed the bands observed on alumina along with a very intense band at 1552 cm^{-1}. Idriss et al. [6] also observed bands at 1555–1535 cm^{-1} after the adsorption of acetaldehyde on a Pd/CeO$_2$ catalyst and they attributed them to acetate species. It seems that the presence of Pd favors the formation of such acetate species, even at room temperature. As the temperature was raised, the intensity of the bands originally observed at room temperature decreased while the intensity of the bands at 1463 and 1582 cm^{-1} increased. Once again, these bands are attributed to the formation of acetate species. However, this time the temperature was raised up to 773 K and a maximum in the intensities of the bands related to the acetate species was observed around 573 K. The results also showed the appearance of bands at 2232 and 2263 cm^{-1} after 473 K. The nature of these features is not very clear. However, while studying the interaction of CO with Pd on Pd/Al$_2$O$_3$ catalysts, Tessier et al. [18] observed IR bands between 2234 and 2245 cm^{-1}, which they attributed to Al^{3+}–C≡O species. A similar result was also obtained by Valden et al. [19], who observed a band at 2253 cm^{-1} in the IR spectrum of CO adsorption on alumina. According to those authors, this band may be related to the CO σ bond with strong Lewis acid sites, and they suggested that the complex corresponding to this band would be Al^{3+}–CO. Therefore, it is possible that the bands at 2232 and 2263 cm^{-1} observed in this work are also related to the Al^{3+}–CO complex, which would be formed from the decomposition of the acetate species.

The IR spectra after adsorption of acetaldehyde on the 8Mo and Pd8Mo samples are shown in Figs. 3 and 4. At room temperature, the intensity of the bands related to adsorbed species on alumina (Fig. 1) are drastically decreased due to the fact that the molybdenum oxide partially covers the alumina surface [9]. Furthermore, the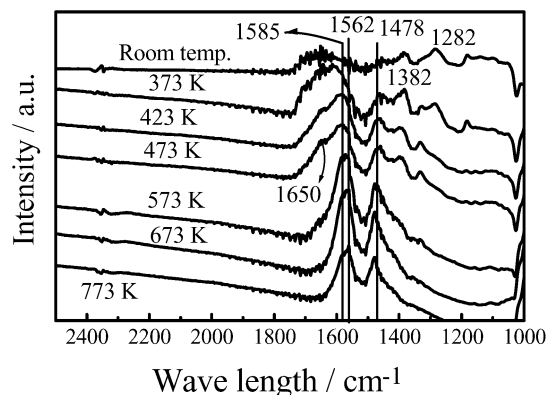se bands were not observed at all for the Pd8Mo catalyst; instead, the bands related to acetate species (1474 and 1574 cm^{-1}) were present even at room temperature (Fig. 4). This indicates that the presence of Pd along with Mo greatly favors the formation of such stable species on adsorption of acetaldehyde. As the temperature was raised, the bands around 1478 and 1585 cm^{-1} increased up to 573 K and decreased after that. On the other hand, bands appeared at 1650 and 1562 cm^{-1}. The nature of these bands remains unclear, but they have been tentatively associated with acetate species adsorbed on the surface of partially reduced molybdenum oxide.
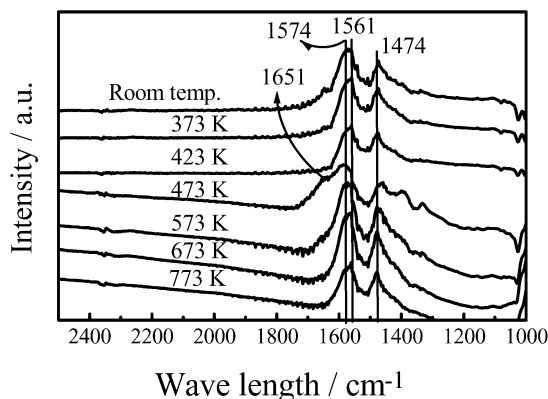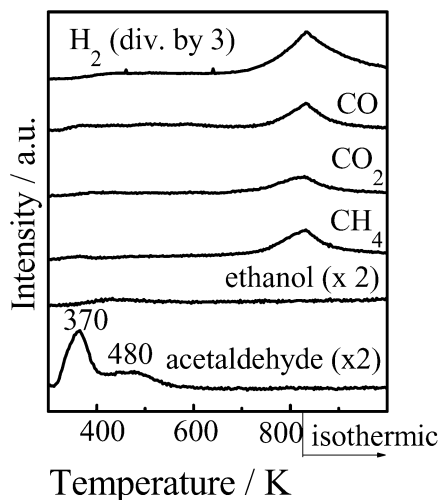
It was impossible to obtain FTIR data for the catalysts containing high concentrations of Mo (20Mo and Pd20Mo), because there was no transmittance through the reduced samples.

3.3. Acetaldehyde TPD

The TPD results after adsorption of acetaldehyde on alumina and the Pd/alumina catalyst are presented in Figs. 5 and 6, respectively. For the support, the desorption of acetaldehyde was observed at around 365 K, and a small amount of ethanol was formed at 400 K. Above 700 K, simultaneous formation of CO$_2$, CH$_4$, H$_2$, and CO was detected. In the presence of Pd, the TPD profile was very similar (Fig. 6), with the main difference being the dramatic increase in CO and H$_2$ formation at high temperatures.

Figs. 7 and 8 show the acetaldehyde TPD results for the 8Mo and Pd8Mo catalysts. The profiles are very similar, showing
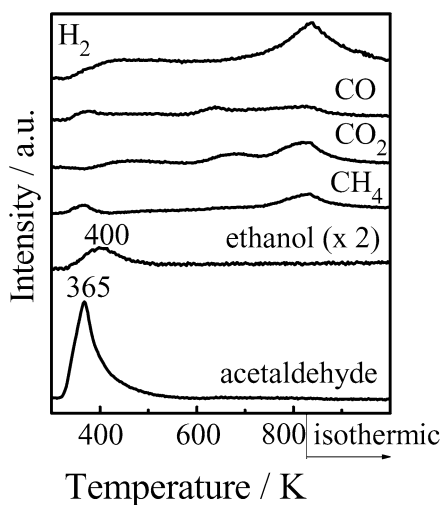
Fig. 5. TPD profile of adsorbed acetaldehyde on Al_2O_3.
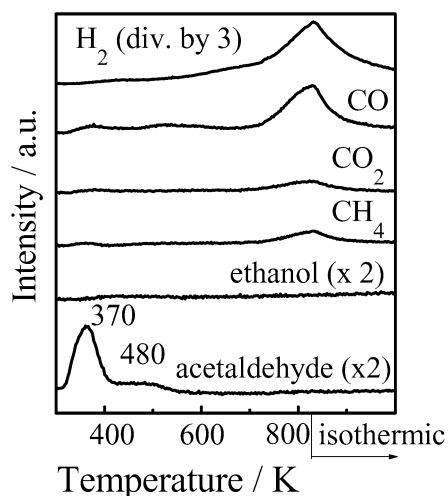
Fig. 8. TPD profile of adsorbed acetaldehyde on $Pd8Mo/Al_2O_3$.
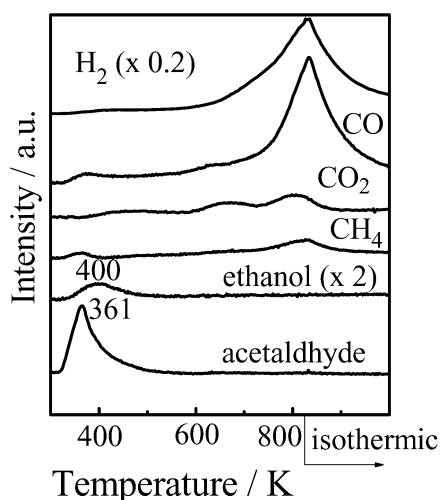
Fig. 6. TPD profile of adsorbed acetaldehyde on Pd/Al_2O_3.
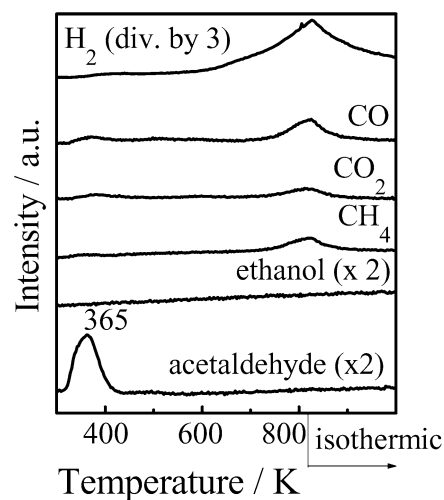
Fig. 9. TPD profile of adsorbed acetaldehyde on $20Mo/Al_2O_3$.

Fig. 7. TPD profile of adsorbed acetaldehyde on $8Mo/Al_2O_3$.

presence of Mo. One possible explanation for the second acetaldehyde peak is adsorption of acetaldehyde on the partially reduced molybdenum oxide. Another distinct feature of these samples is the absence of ethanol formation. Somehow the presence of molybdenum hampered the reduction of acetaldehyde to ethanol, which was a characteristic reaction of the alumina support. Once again, the simultaneous formation of CO_2, CH_4, H_2, and CO at high temperature was observed; apparently, the presence of Pd on the Pd8Mo sample seems to favor the formation of CO and H_2 only when compared with the 8Mo catalyst. This behavior is similar to that observed for the alumina and Pd/Al_2O_3 catalysts, although it was less intense for the 8% Mo-containing pair of catalysts.

For the 20% Mo-loading catalysts (Figs. 9 and 10), the TPD profiles after adsorption of acetaldehyde were practically identical and, again, there was no formation of ethanol. However, two interesting facts can be pointed out. First. unlike the catalysts containing 8% Mo (Figs. 7 and 8), there was only one peak of acetaldehyde desorption, at around 365 K. Therefore, it is not likely that the second acetaldehyde peak observed for the 8Mo and Pd8Mo samples are related to the adsorption on partially re-
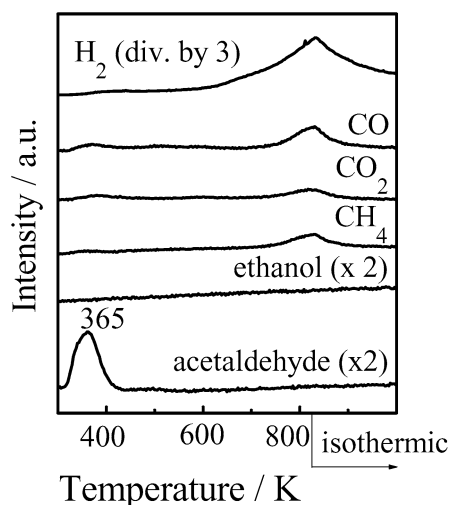
the desorption of unreacted acetaldehyde at 370 and 480 K. This second peak was not observed on the TPD profiles of Al_2O_3 and Pd/Al_2O_3 (Figs. 5 and 6) and appeared only in the

Fig. 10. TPD profile of adsorbed acetaldehyde on Pd20Mo/Al$_2$O$_3$.

Fig. 11. TPSR profile of NO + acetaldehyde on 8Mo/Al$_2$O$_3$.

Fig. 12. TPSR profile of NO + acetaldehyde on Pd/Al$_2$O$_3$.

duced molybdenum oxide, as mentioned before. Second, even though Pd was present on the Pd20Mo sample, there was no increase in CO and H$_2$ formation at high temperatures compared with in the 20Mo catalyst. This behavior differs from that seen for the pairs Al$_2$O$_3$–Pd/Al$_2$O$_3$ (Figs. 5 and 6) and 8Mo–Pd8Mo (Figs. 7 and 8).

3.4. TPSR

The acetaldehyde + NO TPSR result for the 8Mo catalyst is presented in Fig. 11. Acetaldehyde desorbed at 370 and 500 K, with a shoulder at around 350 K, whereas ethanol was seen at around 400 K. NO consumption began only above 600 K, with a simultaneous increase in the intensity of the signal $m/e = 28$ (possibly related to N$_2$ and/or CO formation). This consumption increased until the temperature reached the upper limit of 823 K, at which point the temperature was kept constant, thus decreasing the NO reaction. The intensity of the signals $m/e = 12$ and 44 (related with CO$_2$ formation) showed a similar profile, presenting two weak peaks, one at around 685 K and the other at 823 K (due to the lack of temperature increase).

Fig. 12 shows the acetaldehyde + NO TPSR profile for the Pd/Al$_2$O$_3$ catalyst. A small amount of acetaldehyde desorption was detected in two peaks (at 375 and 485 K), but no ethanol formation was observed. The NO uptake showed two consumption peaks at around 630 and 775 K. Both peaks were followed by increased signal intensity $m/e = 28$, 44, and 12. These signals may represent the formation of N$_2$ ($m/e = 28$), CO ($m/e = 28$ and 12), and/or CO$_2$ ($m/e = 44$, 28, and 12).

The TPSR results for the Pd8Mo catalyst are shown in Fig. 13. A very small amount of acetaldehyde desorbed at 395 and 485 K, and no ethanol was formed. NO consumption also began above 570 K, showing a strong peak around 645 K and a shoulder around 730 K. The peak at 645 K was followed by a sharp increase in the intensity of the signals $m/e = 28$, 44, and 12. The signal $m/e = 28$ also presented an unresolved peak at around 730 K, whereas the intensity of the signals
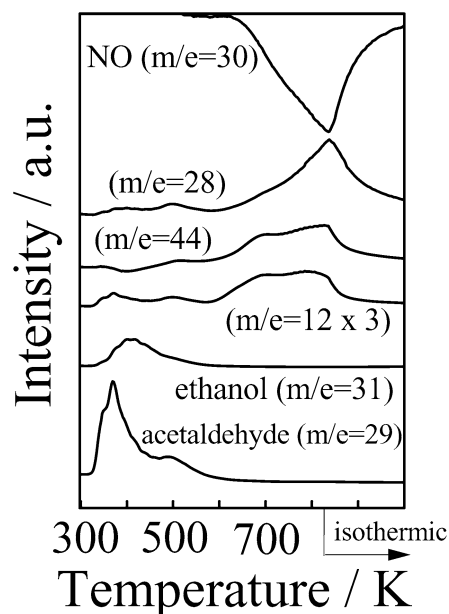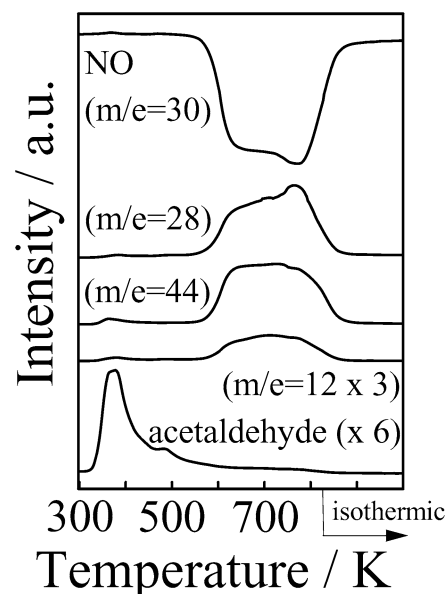
$m/e = 44$ and 12 diminished very slowly with increasing temperature.

3.5. Catalytic activity

Table 4 gives the conversion and selectivity results obtained for the NO + acetaldehyde reaction. The Pd8Mo catalyst was the most active, with higher NO and acetaldehyde conversions. The 8Mo catalyst was not active for converting NO, and only acetaldehyde decomposition was observed. The only nitrogen-containing products detected were N$_2$ and N$_2$O, and for higher NO conversion levels, the selectivity for nitrogen formation was approximately the same on all samples. For lower conversions, the Mo-containing catalysts showed bet-

Fig. 13. TPSR profile of NO + acetaldehyde on Pd8Mo/Al$_2$O$_3$.

Table 4
NO and acetaldehyde conversion and product selectivity for the NO + acetaldehyde reaction

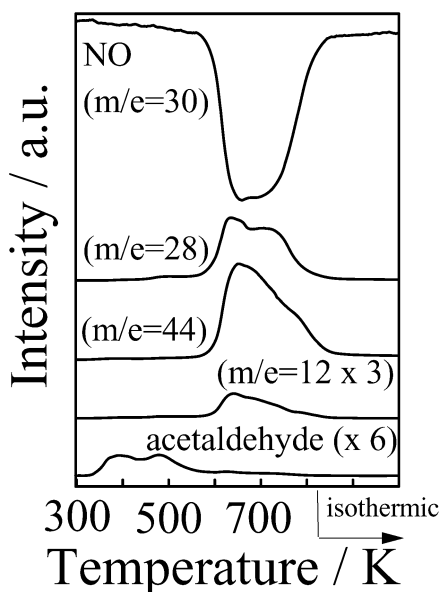| Catalyst	Temperature (K)	NO conversion (%)	N$_2$ selectivity (%)	Conversion acetaldehyde (%)	Selectivity for carbon-containing species (%)	
					CO	CO$_2$
Pd	553	2	50	17.5	65	35
	573	11.5	67	21	50	50
	593	35.5	69	28	29	71
	623	69	69	44	27	73
	673	85	71	62	31	69
Pd8Mo	553	8	79	28	73	27
	573	25	68	43	40	60
	593	53	67	64	37	63
	623	79	63	84	41	59
	673	90	65	93	32	68
Pd–20Mo	553	0	–	9	11	89
	573	6	100	12	25	75
	593	23	70	14	30	70
	623	37	67.5	17	40	60
	673	59	77	30	41	59
8Mo	553	–	–	–	–	–
	573	0	–	39	0	100
	593	0	–	52	0	100
	623	0	–	59	1	99
	673	0	–	69	7	93

ter N$_2$ selectivity. For the catalysts containing Pd, as the reaction temperature increased, so did the selectivity for CO$_2$ formation, indicating more complete oxidation of acetaldehyde.

Table 5 characterizes the effect of adding oxygen to the feed. Pd8Mo catalyst exhibited higher NO conversion as previously observed on the catalytic experiment in absence of oxygen. NO conversion was also not detected on the 8Mo catalyst. On the other hand, the acetaldehyde conversion was practically the same on both Pd8Mo and Pd catalyst. Concerning the selectiv-

Table 5
Effect of oxygen addition to the feed

Catalyst	Temperature (K)	NO conversion (%)	N$_2$ selectivity (%)	Conversion acetaldehyde (%)	Selectivity for carbon-containing species (%)	
					CO	CO$_2$
Pd	553	7	33	43	43	57
	593	18	35	78	4	96
	673	45	48	100	0	100
Pd8Mo	553	7	48	38	37	63
	593	37	29	69	10	90
	673	80	55	100	5	95
Pd–20Mo	553	3	46	18	21	79
	593	8	71	26	37	63
	673	56	73	71	18	82
8Mo	553	0	–	42	0	100
	593	0	–	64	6	94
	673	8	86	83	19	81

ity to nitrogen-containing products, the N$_2$ formation increased with increasing Mo content.

4. Discussion

The results presented above are a continuation of a line of work studying the alumina-supported Pd–Mo catalysts. Previously published papers [9–13] have thoroughly investigated the NO, CO, and ethanol adsorption properties and reaction mechanisms on these catalytic systems, which we find important and relevant for the discussion and conclusions drawn here. Thus we make frequent reference to these works throughout the discussion.

4.1. Acetaldehyde adsorption

The TPD results of adsorbed acetaldehyde on alumina (Fig. 5) showed that part of the acetaldehyde was adsorbed reversibly, as indicated by the peak at 365 K. However, a small part of the acetaldehyde was reduced to ethanol, which was observed at 400 K. Cordi and Falconer [5] studied the adsorption properties of some volatile organic compounds on alumina-supported Pd catalysts and found no ethanol formation on TPD of adsorbed acetalhdehyde on alumina. However, they did observe the formation of CO, CO$_2$, and H$_2$ above 450 K. On the other hand, Idriss et al. [6] detected ethanol formation at 390 and 470 K during acetaldehyde TPD on CeO$_2$; when Pd was added, they observed the formation of ethanol only at 400 K. The IR results presented here (Fig. 1) show the presence of ethoxy species at room temperature. The intensity of these species decreased rapidly with increasing temperature, indicating that they may be the precursors of ethanol formation. In fact, according to Idriss et al. [6], the reduction of acetaldehyde to ethanol is due to hydrogen incorporation on the acetaldehyde species adsorbed. Moreover, it has been suggested [8] that the reduction of acetaldehyde to form adsorbed ethoxy species might be the product of proton abstraction from surface OH groups. These facts indicate that part of acetaldehyde

adsorbed, forming ethoxy species, and that with increasing temperature, a fraction of the acetaldehyde simply desorbed (i.e., reversibly adsorbed acetaldehyde) and another fraction reacted, producing ethanol, as observed during TPD analyses on alumina (Fig. 5). Furthermore, the intensity of the band related to the carbonyl group of adsorbed acetaldehyde (1705 cm^{-1}) decreased, whereas the intensity of the bands related to acetate species (1465 and 1580 cm^{-1}) increased. It is clear that with increasing temperature, acetate species were formed. Such species were more stable and remained adsorbed until higher temperatures were reached. Above 700 K, they probably decomposed and/or reacted with surface hydroxyls to form CO_2, CO, CH_4, and H_2. These results are in agreement with previously reported results for ethanol adsorption/reactions [12,13].

Apparently, the main effect of adding Pd to alumina was the increased CO and H_2 formation at high temperatures during TPD. This result is similar to that reported by Cordi and Falconer [5] during TPD of adsorbed acetaldehyde on a Pd/Al_2O_3 catalyst. The IR results for acetaldehyde adsorption on the Pd catalyst demonstrate that the presence of the metal also seemed to favor the formation of acetate species. As the surface was heated, the intensity of the bands related to the more stable species (at 1463 and 1582 cm^{-1}) increased, reaching a maximum at around 573 K, again suggesting that the acetate species decomposed at higher temperatures. However, the TPD profile of adsorbed acetaldehyde on the Pd catalyst (Fig. 6) shows CO and H_2 evolution only above 650 K. On the other hand, IR analysis shows that bands at 2232 and 2263 cm^{-1} appeared at around 473 K and reach a maximum of intensity at 673 K; these are possibly related to an Al^{3+}–C≡O complex [18,19]. These results suggest that in the presence of Pd, as the acetate species decomposed, the decomposition products (CO and H_2) probably adsorbed on the Pd sites and diffused to the alumina surface, characterizing a spillover-like phenomenon [20]. However, it is important to stress that the apparent stability of this Al^{3+}–C≡O species at this high temperature is quite surprising, and additional studies must be carried out to confirm this attribution. At temperatures above 650 K, CO and H_2 begin to desorb and CO_2 may be formed by the reaction of CO with surface hydroxyls.

For the Mo-containing catalysts, TPD revealed no ethanol formation. The incorporation of MoO_3 probably covered a great part of the alumina surface, thus hampering the reduction of acetaldehyde to ethanol by the oxide hydroxyls. However, complete coverage of the alumina support for the 8% Mo catalysts was not reached, because the monolayer of MoO_x on alumina is formed above 8% of Mo [9,10]. As expected, the IR results show the presence of ethoxy species on the alumina surface, mainly on the 8Mo sample, although the intensity of the bands was lower than on Al_2O_3 and Pd/Al_2O_3. As mentioned before, these ethoxy species are probably the precursors for ethanol formation, which occurs at around 400 K during TPD on both alumina and the Pd catalyst. However, for the 8Mo and Pd8Mo samples, ethanol formation was not seen, and a second peak of acetaldehyde was observed at 480 K. The presence of molybdenum oxide may have made the reduction of such ethoxy species more difficult, causing it to simply desorb as acetaldehyde at higher temperatures. For the catalysts containing 20% Mo, the

monolayer of MoO_x on alumina was formed and bulk MoO_x, not allowing the adsorption and formation of ethoxy species on the alumina surface to begin with. This would explain the absence of either ethanol formation or a second peak of acetaldehyde desorption during TPD analyses on these samples.

Once again, the presence of Pd on the Pd8Mo catalyst favored the formation of more stable acetate species (compared to the 8Mo sample). However, it is noteworthy that in this case, the acetate species were formed even at room temperature. This result was not observed after Pd incorporation on alumina and suggests that the presence of partially reduced molybdenum oxide in intimate contact with palladium particles greatly favors and stabilizes such acetate species.

In a previous work [9], it was shown through TPR experiments on Pd–Mo/Al_2O_3 catalysts that the presence of Pd promotes the reduction of MoO_3. Therefore, the Pd–Mo samples contain a greater amount of MoO_x species (partially reduced molybdenum oxide) than the Mo-only samples. But comparing the TPD profiles of the 8Mo and 20Mo samples with those of the Pd8Mo and Pd20Mo samples reveals no significant differences except for the greater amount of CO and H_2 at higher temperature on the Pd8Mo sample and the absence of a second peak of acetaldehyde on the high Mo-loading samples. This suggests that the higher concentration of MoO_x species on the Pd-containing samples does not extensively influence the adsorption and decomposition of acetaldehyde. This phenomenon was also observed when ethanol adsorption properties were studied on Pd–Mo–Al_2O_3 [12]. However, this is in contrast to what was observed previously for the adsorption of CO and NO on Pd–Mo/Al_2O_3 catalysts [9–11]. In this case, the higher amount of partially reduced molybdenum oxide increased the adsorption and decomposition of both CO and NO. (In the case of NO, it greatly improved the decomposition to N_2.)

Another interesting point is that adding Pd to the 20Mo catalyst did not increase CO and H_2 formation at high temperature as it did for the Pd and Pd8Mo catalysts during TPD of adsorbed acetaldehyde. A similar result was also observed when studying the effect of high Mo concentration on the adsorption properties of CO, NO, and ethanol on Pd–Mo/Al_2O_3 catalysts [9,11,12]. This is due to the fact that when 20% Mo concentration is used, bulk MoO_3 is formed [9] and these crystalline species may cover part of the Pd particles. This is in agreement with the H_2 chemisorption results shown in Table 3, which show that H_2 uptake for the Pd20Mo sample was approximately the same as for the 20Mo catalyst (approximately 42 times lower than on Pd/Al_2O_3).

4.2. NO + acetaldehyde reaction

The NO + acetaldehyde TPSR profiles for the Pd/Al_2O_3 and Pd8Mo/Al_2O_3 catalysts were very similar. Basically, NO consumption was followed by an increased intensity of the signals $m/e = 44$, 28, 12. This suggests that N_2, N_2O, CO, and CO_2 may have been formed. Because the intensity of the signal $m/e = 12$ increased simultaneously to the signals $m/e = 28$, 44, it is reasonable to conclude that both CO and CO_2 were formed. This result indicates that NO reacts with adsorbed

carbon-containing species at temperatures above 570 K. Furthermore, comparing the TPSR results (Figs. 12 and 13) and TPD results (Figs. 6 and 8) is made, it can be easily seen that the profiles below 550 K are very similar, whereas above 550 K it is completely different, indicating that product formation on TPD is due to decomposition of adsorbed species while on TPSR it is due to the reaction of adsorbed species with NO. However, as revealed by IR analyses, only acetate species were detected at the temperature range where NO was consumed on the TPSR experiment. The other possible surface species detected upon adsorption of acetaldehyde at room temperature are not stable above 570 K. Therefore, this suggests that the acetate species are the carbon-containing species that react with NO during TPSR. This same conclusion was achieved in a previous work when the NO + ethanol reaction was investigated over Pd–Mo/Al$_2$O$_3$ catalysts [12]. In fact a reaction mechanism was proposed for the ethanol + NO reaction [12] and according to this mechanism, NO adsorbs preferentially on the Pd particles while ethanol adsorbs as ethoxy species on alumina and/or partially reduced molybdenum oxide. The ethoxy species are dehydrogenated to acetaldehyde which is immediately oxidized to acetate species at the reaction temperature. After that, the acetate species react with NO at the metal/oxide interface. Furthermore, catalytic activity measurements suggested that the dehydrogenation of ethanol to acetaldehyde was the rate-limiting step for this reaction [12].

Although very similar observations were made regarding ethanol and acetaldehyde adsorption properties on the catalytic systems studied here, the catalytic activity measurements on NO + ethanol and NO + acetaldehyde reactions revealed important differences.

In the case of NO + ethanol reaction [12], the conversion followed the order: Pd/Al$_2$O$_3$ > Pd8Mo > Pd20Mo > 8Mo and 20Mo (no activity). Therefore, it seems that the addition of molybdenum oxide to the palladium catalyst decreased the NO conversion, which indicates that the main reaction step takes place at the Pd sites. Once again, it is important to emphasize that according to this mechanism, NO adsorbs on Pd particles, and the ethanol dehydrogenation to acetaldehyde is the rate-limiting reaction step.

In the present work, it was observed that at the reaction temperature, acetaldehyde was readily oxidized to acetate species, which were the only stable surface species present. As stated above, these are the carbon-containing species that react with NO at the metal oxide interface. However, unlike the ethanol + NO reaction [12], the acetate species here were readily formed on contact of acetaldehyde with the catalytic surface. In other words, the NO + acetaldehyde reaction was not limited by the ethanol dehydrogenation step. This had a strong effect on the NO conversion, as shown in Table 4.

Instead of decreasing NO conversion, Mo addition promoted it. Pd8Mo was the most active catalyst. In fact, the presence of partially reduced molybdenum oxide favored the formation of acetate species, as observed on the IR spectrum of Pd8Mo catalyst, even at room temperature. This explains the higher activity of Pd8Mo compared with Pd/Al$_2$O$_3$.

Furthermore, NO conversion on the NO + acetaldehyde reaction was higher than on the NO + ethanol reaction, due to the presence of higher concentrations of acetate species at the metal–oxide interface. In the case of NO + ethanol reaction, the rate of acetate formation depended on the rate-limiting acetate formation step.

Another interesting fact is that the selectivity for N$_2$ formation during the reaction was approximately the same on all catalysts (except at low temperatures), regardless of the presence of Mo, indicating that the reaction pathway was the same on all samples. This was also observed for the NO + ethanol reaction.

For purposes of comparison, the ethanol + NO reaction as proposed previously is reproduced below, as follows [12]:

– NO adsorbs preferentially on Pd particles while ethanol adsorbs dissociatively, forming adsorbed ethoxy species:

$$[NO + Pd \rightarrow NO\text{–}Pd], \tag{1}$$

$$[CH_3CH_2OH + 2S \rightarrow CH_3CH_2O\text{–}S + H\text{–}S]. \tag{2}$$

– At the reaction temperature, the ethoxy species are dehydrogenated, providing the overall dehydrogenation of ethanol to acetaldehyde:

$$[CH_3CH_2O\text{–}S + H\text{–}S \rightarrow CH_3CHO + H_2 + 2S]. \tag{3}$$
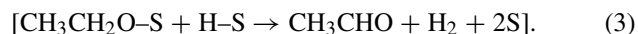
– At the reaction temperature, acetaldehyde is readily activated, leading to intermediate acetate species:

$$[CH_3CHO + S + NO\text{–}Pd \xrightarrow{[O]} CH_3COO\text{–}S + HNO\text{–}Pd]. \tag{4}$$
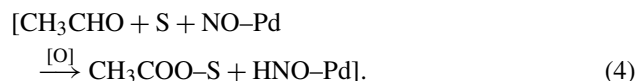
– Reaction between adsorbed species then proceeds at the metal–oxide interface:

$$NO\text{–}Pd + 2HNO\text{–}Pd + 2CH_3COO\text{–}S \xrightarrow{-[O]} 5N_2 + 4CO_2 + 4H_2O + 2S + 10Pd, \tag{5}$$
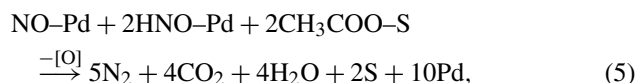
where [O] represents surface oxygen.

Based on the results presented here, and taking into account the reaction mechanism proposed previously for the NO + ethanol reaction [12] as reproduced above, we believe that the reaction mechanism for NO + acetaldehyde involves the following steps:

$$[NO + Pd \rightarrow NO\text{–}Pd], \tag{6}$$

$$[CH_3CHO + S + NO\text{–}Pd \xrightarrow{[O]} CH_3COO\text{–}S + HNO\text{–}Pd], \tag{7}$$

$$NO\text{–}Pd + 2HNO\text{–}Pd + 2CH_3COO\text{–}S \xrightarrow{-[O]} 5N_2 + 4CO_2 + 4H_2O + 2S + 10Pd, \tag{8}$$
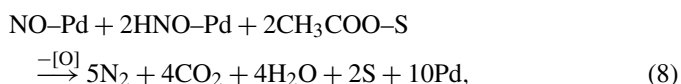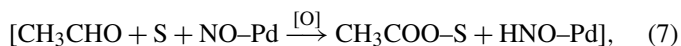
where [O] represents surface oxygen and S = empty site (Al$_2$O$_3$ or MoO$_x$).

NO molecules adsorb on metallic palladium sites (step (6)), whereas acetaldehyde adsorbs on alumina (in case of Pd/Al$_2$O$_3$) and/or partially reduced molybdenum oxide (in case of Pd–Mo

samples) and is readily activated, leading to acetate species as shown in step (7). Step (8) represents the reaction of adsorbed species at the metal–oxide interface. The main difference from the NO + ethanol reaction is the absence of steps (7) and (8).

As discussed above, because the rate-limiting step of ethanol dehydrogenation does not occur for the NO + acetaldehyde reaction, and also because the presence of both Pd and MoO_x favors the presence of active acetate species, the Pd–Mo catalyst is expected to be more active than the Pd-only catalyst. This in fact is what happened when 8% Mo was added. Nevertheless, the Pd20Mo catalyst was less active than the other Pd-containing catalysts. This may be due to the fact that at such high Mo loading, bulk MoO_x crystallites prevail at the surface, covering the major part of the Pd particles and hampering the NO adsorption on Pd and, thus, the reaction itself. A similar result was also seen before for the reaction of NO with ethanol on high Mo loading Pd–Mo catalysts [11,12].

The addition of oxygen decreased the NO conversion, but increased acetaldehyde conversion and CO_2 selectivity. Actually, two competing reaction routes may have occurred: (i) acetaldehyde oxidation by oxygen from the feed and (ii) acetaldehyde reaction with NO, which follows the reaction scheme previously described. The direct oxidation of acetaldehyde was favored on Pd/Al_2O_3, whereas NO reduction with acetaldehyde occurred mainly on Pd8Mo. These results are in agreement with the proposed reaction mechanism, taking into account that oxygen adsorbs on Pd and MoO_x sites. Therefore, oxygen has a much greater effect on NO adsorption on Pd/Al_2O_3, explaining the lower NO conversion on this catalyst.

Finally, taking into account our previous work on NO + CO and NO + ethanol reactions, together with the study of NO + acetaldehyde reaction, we can establish important guidelines for designing catalysts for emissions control from fuels containing oxygenated compounds, such as ethanol. The presence of an oxide with redox properties is necessary to promote the CO + NO reaction. This oxide will also increase the formation of acetate species, which is the intermediate on the NO + oxygenated compound reactions. On the other hand, the addition of this oxide cannot reduce the exposed surface of the noble metal, because these are the sites responsible for NO adsorption.

5. Conclusion

The reduction of NO with acetaldehyde on alumina-supported Pd, Mo, and Pd–Mo catalysts was studied. TPD and IR measurements of adsorbed acetaldehyde indicated that the presence of Pd and Mo changed the adsorption properties of

acetaldehyde. An important result was that the presence of Pd in close contact with Mo greatly favored the formation of acetate species, which are probably important reaction intermediates. This finding could explain the higher activity presented by the Pd8Mo sample for the conversion of NO during the NO + acetaldehyde reaction. The 20% Mo loading produced bulk MoO_3, which covered part of the Pd sites; thus, the activity for this catalyst was lower. Another interesting fact was that the selectivity for N_2 formation during the reaction was the same on all catalysts (except at low temperatures) regardless of the presence or absence of Mo, indicating that the reaction pathway was the same on all samples. A mechanism has been proposed in which the NO adsorbs preferentially on the metallic Pd sites and the acetaldehyde adsorbs mainly on the surfaces of alumina and/or partially reduced molybdenum oxide, leading to acetate species. The reaction occurs between the intermediate acetate species and the adsorbed NO.

Acknowledgment

References

[1] J.N. Armor, Appl. Catal. B Environ. 1 (1992) 221.
[2] D.A. Guerrieri, P.J. Caffrey, V. Rao, SAE Paper 950777 (1995) 85.
[3] E.W. Conti, D.R.M. Pomaleski, M.L. Brandão, Proceedings of the VII SIMEA (1993) 38.
[4] A.P. Altshuller, Atmos. Environ. A 27 (1993) 21.
[5] E.M. Cordi, J.L. Falconer, J. Catal. 162 (1996) 104.
[6] H. Idriss, C. Diagne, J.P. Hindermann, A. Kiennemann, M.A. Barteau, J. Catal. 155 (1995) 219.
[7] M. Nagal, R.D. Gonzalez, Ind. Eng. Chem. Prod. Res. Dev. 24 (1985) 525.
[8] J. Raskó, J. Kiss, Appl. Catal. A Gen. 287 (2005) 252.
[9] M. Schmal, M.A.S. Baldanza, M.A. Vannice, J. Catal. 185 (1999) 138.
[10] F.B. Noronha, M.A.S. Baldanza, M. Schmal, J. Catal. 188 (1999) 270.
[11] M.A.S. Baldanza, L.F. de Mello, A. Vannice, F.B. Noronha, M. Schmal, J. Catal. 192 (2000) 64.
[12] L.F. Mello, F.B. Noronha, M. Schmal, J. Catal. 220 (2) (2003) 358.
[13] L.F. Mello, M.A.S. Baldanza, F.B. Noronha, M. Schmal, Catal. Today 85 (2003) 3.
[14] A.H. Miguel, J.B. Andrade, J. Braz. Chem. Soc. 1 (1990) 124.
[15] J.E. Benson, H.S. Hwang, M. Boudart, J. Catal. 30 (1973) 46.
[16] A. Yee, S.J. Morrison, H. Idriss, J. Catal. 186 (1999) 279.
[17] R.G. Greenler, J. Chem. Soc. 82 (1962) 2488.
[18] D. Tessier, A. Rakai, F. Bozon-Verduraz, J. Chem. Soc. Faraday Trans. 88 (1992) 741.
[19] M. Valden, R.L. Keiski, N. Xiang, J. Pere, J. Aaltonen, M. Pessa, T. Maunula, A. Savimäki, A. Lahti, M. Härkönen, J. Catal. 161 (1996) 614.
[20] C. Li, Q. Xin (Eds.), Spillover and Migration of Surface Species on Catalysts, Studies in Surface Science and Catalysis, vol. 112, Elsevier Science, Amsterdam, 1997.